

Non-Doppler Broadening Mechanisms of CXRS-Emission Profiles and their Contributions to Ion Temperature Measurements

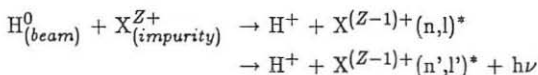
J. V. HOFMANN, G. FUSSMANN

Max-Planck-Institut für Plasmaphysik
D-8046 Garching, West Germany

We discuss various broadening mechanisms on emission profiles in the UV and visible range resulting from charge exchange recombination (CXR) reactions. In particular, broadening contributions from fine structure splitting, Zeeman - and Stark effects are calculated for Kr^{25+} and O^{7+} ions to deduce ion temperatures in ASDEX.

1. Introduction

During the last years charge exchange recombination spectroscopy has been developed to a very successful diagnostic tool in tokamak devices where high energy neutral injectors are applied for additional heating. Especially the UV and visible range experienced a renaissance because of apparative advantages and the possibility to substantiate fully stripped ions in the plasma core providing important information on the plasma ion temperature, plasma rotation velocity and impurity concentrations. The charge exchange reaction



leads to photon emission in the UV and visible range which is most suitable for ion temperature measurement based on the Doppler broadening of the profiles. The emission results from $\Delta n = 1$, $\Delta l = 1$ transitions of highly excited Rydberg states $(n',l')^*$. In this context we do not consider possible - but generally small - deviations between the temperatures of background and impurity ions [1] but concentrate on atomic physics aspects. Specifically contributions from fine structure splitting of the generally unresolved l-levels of a transition, the Zeeman splitting in the magnetic field of the tokamak and the translational Stark effect due to the $\vec{v} \times \vec{B}$ field of the ions may have a non negligible influence on the total broadening depending on the investigated impurity and the observed transition.

We elucidate these effects by referring to H-like O^{7+} and Na-like Kr^{25+} which are sufficiently different in mass and charge. The visible transitions of these two ions and their population structures have been carefully analysed in ASDEX [2,3].

2. Fine Structure Contributions

We first calculate the intensities of all $\Delta l = \pm 1$ transitions within an observed $\Delta n = 1$ emission line. An example is shown in Fig. 1 where these intensities are plotted as a function of wavelength λ for the measured Kr^{25+} transition $n = 17-16$ ($\lambda =$

302.11 nm). As expected, the emission is dominated by the $\Delta l = -1$ transitions (labeled o) originating from the highest l-states. The $\Delta l = +1$ transitions are much smaller in intensity (see logarithmic insert). The fine structure for H-like O^{7+} is obtained from the well-known relation

$$E_{nj} = E_n^0 + \Delta E_{nj} = E_n^0 \left(1 + \frac{(Z\alpha)^2}{n} \left(\frac{1}{j+1/2} - \frac{3}{4n} \right) \right)$$

with $E_n^0 = -(Z\alpha)^2 \cdot mc^2 / (2n^2)$, $\alpha = e^2 / (4\pi\epsilon_0 \cdot \hbar c)$, $j = l \pm 1/2$. For the lower j-levels of Kr^{25+} which, however, contribute very little to the total intensity this formula cannot be used. The numerical calculations are based on a code by Summers [4].

Next we assign to each transition a Doppler profile and obtain by superposition the total emission profile shown in Fig. 2 (labeled as o). To this profile we fit a single Gaussian to deduce a fit temperature. According to our measurements we choose Poisson statistics for the weight of the datapoints. The resulting fit, which is very close to the data in the core region, is the solid curve in Fig. 2. However, as can be seen, some deviations remain in the wings of the profile.

Applying this procedure for several temperatures as input ($T = 0.5-6$ keV), our calculations yield a linear dependence between true and fit temperatures with a slope very close to 1 but with a positive off-set for the fit temperature. For the $n = 17-16$ transition of Kr^{25+} this off-set is as large as $T_{fit} - T_{true} = 1.7$ keV. This clearly demonstrates the importance of the additional fine structure broadening in this case. In the case of the O^{7+} $n = 10-9$ ($\lambda = 606.83$ nm) transition this contribution is markedly reduced to 0.16 keV.

3. Zeeman- and Stark-Effect

The contributions according to Zeeman splitting and translational Stark effect are estimated for ASDEX conditions ($B = 2$ T) for the observed $\Delta n = 1$ transitions (Kr^{25+} : $n=23-22, \dots, 16-15$, O^{7+} : $n=10-9, \dots, 8-7$). Strictly speaking we have to consider the anomalous Zeeman effect for each unresolved fine structure transition which leads to a vasting number of components. However, for high orbital momenta l and $j = l \pm 1/2$ (one electron outside closed shells) the Landé g -factor, $g = 1 + (j(j+1) + s(s+1) - l(l+1)) / (2j(j+1))$, is always close to 1. In this case the anomalous Zeeman effect can be approximated by the normal Zeeman effect yielding triplets with a total energy splitting of $\Delta E = 2 \cdot \mu_B \cdot B$ where μ_B is Bohr's magneton. To a first estimate we take this splitting into account by assuming an additional equivalent Gaussian broadening (typically $\Delta E = 2.3 \cdot 10^{-4}$ eV). After performing the corresponding convolution with the Doppler profile we find a rather small effect on the fit temperature of order 1-3 % for both Kr^{25+} and O^{8+} .

The translational Stark effect is estimated for $B = 2$ T and $T_i = 2$ keV, leading to a characteristic electric fieldstrength of $\mathcal{E} = \sqrt{2E/m} \cdot B = 3.0 \cdot 10^5$ V/m for oxygen. In this case we have to consider a splitting of the degenerate j -levels ($j = l \pm 1/2$) given by

$$\begin{aligned} \Delta E_S(\text{eV}) &= \frac{3}{2} \cdot \frac{\mathcal{E}}{\epsilon_0} \cdot E_0 \cdot \frac{n}{2Z} \cdot \frac{\sqrt{n^2 - (j+1/2)^2}}{j \cdot (j+1)} \\ &= 3.971 \cdot 10^{-11} \cdot \mathcal{E}(\text{V/m}) \cdot \frac{n}{Z} \cdot \frac{\sqrt{n^2 - (j+1/2)^2}}{j \cdot (j+1)} \end{aligned}$$

where $E_0 = 2 \cdot hc/e \cdot Ry = 27.2 \text{ eV}$ and $\mathcal{E}_0 = e/(4\pi\epsilon_0 \cdot a_0^2) = 5.142 \cdot 10^{11} \text{ V/m}$. This yields for example a splitting of the $O^{7+} n = 10, l = 8, j = 17/2$ level of $\Delta E_S(O^{7+}) = 8.039 \cdot 10^{-7} \text{ eV}$ which is only 0.75 % of the fine structure splitting. The splitting increases for the lower j levels and reaches for $j = 1/2$ about 7 % of the fine structure. Conversely, for the highest j component ($j = 19/2$) the Stark splitting is exactly zero since this level is not degenerate. Since the main contribution to our investigated lines originates from the highest l - and j - states we conclude that the Stark effect can indeed be neglected.

4. Results

In *Figs. 3, 4* the several contributions to the ion temperature for the visible krypton and oxygen transitions are plotted. The numerically determined fit temperature (*FIT*) is assumed to be the sum of the various contributions namely Doppler (*D*), fine structure (*FS*), Zeeman (*B*) and apparatus broadening (*A*). Apart from the *FS* contribution, all other terms are known independently. The *FS* term is thus obtained from $T_{FIT} = T_D + T_{FS} + T_B + T_A$. Clearly Doppler broadening dominates in all cases but for the medium *Z* ion Kr^{25+} the contribution of the fine structure is already 24 % of the fit temperature.

A direct comparison of ion temperatures from different ionic species has not yet been performed. Taking the various broadening contributions into account we compare Doppler temperatures for O^{7+} and Kr^{25+} with those deduced from neutron flux measurements. For O^{7+} we find an agreement within the error bars ($2.7 \pm 0.3 \text{ keV}$). In the case of Kr^{25+} however the determined Doppler temperatures (4 keV) are systematically too high by more than 30 %. A possible explanation for this difference could be an underestimation of the fine structure splitting of the lower j -levels. The different scalings of the additional broadening terms with wavelength (see *Figs. 3, 4*) together with our observations on ASDEX suggest the $O^{7+}, n = 10-9$ ($\lambda = 606.83 \text{ nm}$) transition as best suited for ion temperature measurements using CXRS in cases where intensity problems are of minor importance. On the other hand the Kr^{25+} lines may be more suited for rotation measurements because of a more favourable relation between lineshift and broadening.

REFERENCES

- [1] . Fussmann, *Effects on doppler profiles in beamheated plasmas*, JET-R(87)12 (1987)
- [2] J. V. Hofmann, G. Fussmann, G. Janeschitz, *Charge Exchange Spectroscopy (CXRS) of Highly Ionized Ions in ASDEX*, in *DPG - Frühjahrstagung (Düsseldorf, FRG, Feb 29 - Mar 4, 1988)*, IPP III/134, April 1988
- [3] J. V. Hofmann, *Spektroskopische Analyse von Umladungsprozessen hochionisierter Rydberg-Atome am Experiment ASDEX*, Thesis, Technische Universität München, Nov. 22, 1988
- [4] J. Spence, H. P. Summers, *The recombination and level populations of ions: III. The role of charge exchange from neutral hydrogen*, J. Phys. B, Vol 19, 3749-3776 (1986)

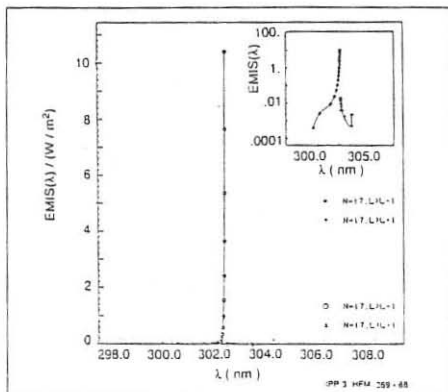


Fig. 1: Contributions of the fine structure components for the $^{36}\text{Kr}^{25+}$ $n = 17-16$ ($\lambda = 302.11$ nm) transition. The $\Delta l = -1$ transitions are labeled \circ , the $\Delta l = +1$ transitions, only to be seen in the logarithmic insert, are labeled Δ .

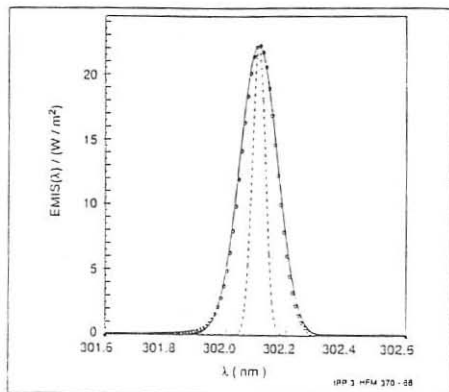


Fig. 2: Complete line profile of the Kr^{25+} $n = 17-16$ transition shown in Fig. 1 including all Doppler broadened fine structure components (dotted curve). The fitted single Gaussian (solid line) and the apporative profile (dashed line) are also shown.

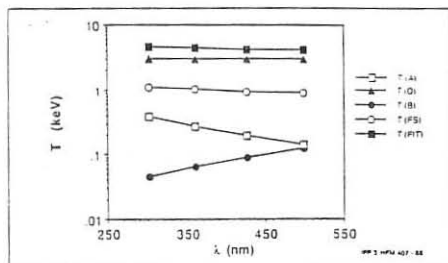


Fig. 3: Contributions to the ion temperature for Kr^{25+} including effects of: apporative profile (A), Doppler broadening (D), Zeeman effekt (B), fine structure (FS) and fit temperature (FIT).

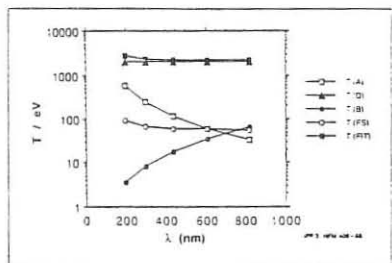


Fig. 4: Contributions to the ion temperature in case of O^{7+} analog to Fig. 3.